Acta Crystallographica Section A
Foundations of Crystallography
ISSN 0108-7673

Received 1 September 1999
Accepted 4 April 2000

Elucidation of simple pathways for reconstructive phase transitions using periodic equi-surface (PES) descriptors. The silica phase system. I. Quartz–tridymite

S. Leoni and R. Nesper*

Laboratorium für Anorganische Chemie, ETH Zürich, Universität Strasse 6, 8092 Zürich, Switzerland. Correspondence e-mail: nesper@inorg.chem.ethz.ch

A method of estimating short topological pathways for solid–solid reconstructive phase transitions is proposed. To screen the simplest pathways out of the infinite manifold in configurational space, a Fourier function approach is used, based on periodic nodal (PNS) and periodic equi-surface (PES) descriptors. The simplicity of the chosen functions representing the structures in question and the linear transition approach provide for most simple relevant transition models. Here it is shown that the tetrahedral networks of quartz and tridymite are represented topologically and transformed into each other by this approach. A trigonal network related to α-$ThSi_2$ and B_2O_3 appears as intermediate during the transition model of the periodic functions. The transition path found in this way seems to be of exciting directness and of fundamental topological interest. The presented approach is not restricted to this specific case and is expected to be applicable to a wide variety of reconstructive phase transitions of solids.

1. Introduction

Reconstructive phase transitions (RPT) are of first-order character and show complicated transition processes that occur when the time correlation between structural domains in space is lost and independent nucleation processes have to take place. Different from second-order transitions, which proceed under strict symmetry control (Landau & Lifshitz, 1959), there is no unequivocal way to define the topology of the transition pathway. In a beautiful monograph, Toledano & Dmitriev (1996) have discussed different approaches to this topic in much detail. Their approach involves a reinspection of the physical meaning of the order parameter and its definition in terms of non-linear periodic functions. A general difference with the Landau theory concerns the form of the order parameter and its relation to a specific geometrical mechanism, which for a particular phase transition is assumed to be of a given type (Toledano & Dmitriev, 1996, p. 171). The last point in particular raises some problems for the generalization of the approach.

Quite recently, Alivisatos *et al.* were able to prove that in some nanocrystals RPT proceed through a single nucleation per particle and thus show cooperative behaviour for each nanoparticle (Chen *et al.*, 1997). In such small domains that transform homogeneously, nature has to solve the topological problem of transforming one structure into another despite the loss of long-range correlations between the domains. For most RPT, the available excitation energies do not allow for an intermediate melting process of larger domains. Although it is clear that the transformation will most likely start at impurities or faults, it has still to travel through the bulk material for the RPT to complete. It is trivial that nature will choose the most economical transition path. However, the question is what does most economical mean? Surely the preferred pathway will utilize low excitation energies but kinetics will play a role as well, *i.e.* a faster RPT pathway with only slightly higher excitation energy will compete with an energetically more favourable but slower one. One important prerequisite of fast kinetics is short displacive and/or diffusive dislocations.

We will try to systematically approach the problem of elucidating simplest pathways by a powerful topological strategy. Such a strategy was worked out with the help of PNS, as they are defined by von Schnering & Nesper (1991). This approach utilizes a Fourier *Ansatz*, which codes the fundamental topological information of a space group or of a specific structure in the form of a short Fourier summation.

A family of surfaces in real space can be generated from a Fourier summation

$$f(x, y, z) = \sum_h \sum_k \sum_l \left|S(hkl)\right| \cos[2\pi(hx + ky + lz) - \alpha(hkl)] \quad (1)$$

according to the expressions

$$\sum_h \sum_k \sum_l \left|S(hkl)\right| \cos[2\pi(hx + ky + lz) - \alpha(hkl)] = 0 \qquad (2)$$

$$\sum_h \sum_k \sum_l \left|S(hkl)\right| \cos[2\pi(hx + ky + lz) - \alpha(hkl)] = \text{constant} \qquad (3)$$

(von Schnering & Nesper, 1991). For $f(x, y, z) = 0$, the resulting surface is called a periodic nodal surface (PNS) because it may have distinct symmetry properties and, for $f(x, y, z) \neq 0$, the surface is a periodic equi-surface (PES) (von Schnering & Nesper, 1985). Both PNS and PES will be called representatives in the following, which means that they represent the topological characteristics of either a space group or a structure (type) or set of structures.

Although an arbitrary number of Fourier coefficients may be chosen, only summations with a small number of structure factors have proven to be useful for the elucidation of the general topological features of a structure or a set of structures of a given symmetry (von Schnering & Nesper, 1991). Selected comparisons of all structure types belonging to a specific space group have shown that very few – in general less than the first ten – structure factors are sufficient to clearly discriminate between the types. In the case of space group No. 227 $Fd\bar{3}m$, only eight structure factors are sufficient for discriminating all types given by the TYPIX database (Parthé, 1995) by their phase permutations only (Leoni, 1998). These small sets of structure factors are not arbitrarily chosen though, but only those (hkl) combinations are considered that arise when systematically starting off from the centre of reciprocal space.

The symbol $S(hkl)$ for the structure factors was used instead of $F(hkl)$, which is meant to indicate that the equation is made independent of any physical quantity like the electron density. The $S(hkl)$ are generated by Fourier transforming a point configuration of dimensionless δ functions. So $S(hkl)$ has the meaning of a geometrical structure factor (von Schnering & Nesper, 1991).

In the following, we will use the expression $\mathbf{S_h}$ not for a single structure factor but for a complete set of equivalent structure factors $S(hkl)$ under a given symmetry. Each set consists of structure factors with reciprocal-lattice vectors $\mathbf{h}$ given by the Laue symmetry related to the space group under consideration and of a set of phases defined by $\alpha(\mathbf{P}^T\mathbf{h}) = \alpha(\mathbf{h}) - 2\pi\mathbf{h}^T\mathbf{t}$ (Shmueli, 1993). $\mathbf{P}$ and $\mathbf{t}$ are the rotation and translation parts of a symmetry operation of the space group. It has been shown that using simple surface representatives allows the generalization of the topological analysis of structures beyond the particular features that each individual structure contains. This requires selection of only one or very few sets $\mathbf{S_h}$ with $|\mathbf{h}|$ as small as possible, but being characteristic for a space group. For example, none of the sets $\mathbf{S_h}$ with $\mathbf{h} = (100)$, (110), (111), (200), (210), (211) or (220) is characteristic for the cubic space group $P\bar{4}3m$ (Laue symmetry $m\bar{3}m$) as a single set because any choice of phases consistent with cubic symmetry will generate representatives that either show a centring or belong to a supergroup. For example, in the case of $\mathbf{h} = (100)$ or (210), the representatives have the symmetry $Pm\bar{3}m$ (von Schnering, 1993).

In the following, structure-factor sets will be characterized by the notation $\mathbf{S_h}(\mathbf{h}, |\mathbf{S_h}|, \alpha)$, $\mathbf{h} = (hkl)$ or ($hkil$), where $\mathbf{h}$ and α refer to only one $S(hkl)$ of the set and i to trigonal or hexagonal metric.

Equations (2) and (3) were the starting point for the definition of simple mathematics and a simple method for the calculation of functions that contain enormous potential for the description and understanding of crystal structures. Numerous examples of such a correlation have been given (Andersson & Jacob, 1997, 1998; Hyde *et al.*, 1997; Leoni, 1998; von Schnering & Nesper, 1987; Oehme, 1989; Zürn, 1998). A few examples of PNS and of the correlation between structures and PNS are given in Fig. 1. PNS and periodic minimal surfaces (PMS) have been shown to be very similar in their spatial coordinates in many cases and the relevance of PMS for the description and understanding of solid-state structures was demonstrated some time ago (Faelth & Andersson, 1982; Andersson *et al.*, 1984). The close relation between the two periodic surface types – though not rigorously proved – is a result of two conditions: (i) they have to obey the same symmetry requirements; (ii) they constitute very smooth and simple functions in the frame of the same symmetry elements if the $\mathbf{h}$ vectors are chosen to be as short as possible (see above).

Among the different ways of correlating crystal structures and PMS, PNS or PES, we mention only some relevant cases: (i) A framework matches the surface in the way that all atoms are on the surface; in other words, the atoms are embedded in the surface. (ii) A structure or partial structure is enveloped by the surface. This allows for the description of a network or atomic arrangement as a labyrinth net (Hyde & Andersson, 1984) of such a periodic surface.

If space is partitioned into two parts that are congruent or transformed into each other by a symmetry operation embedded in the surface, then the surface is called balanced and the groups of the surface and of the labyrinths form a group–subgroup pair of index 2. In the same way, structures on both sides of a balanced surface may be congruent or enantiomers. The latter is a very interesting case occurring for the famous gyroid surface with $Ia\bar{3}d$ symmetry but erroneously assigned to $I4_132$ by its inventor (Schoen, 1970), probably because of the lower symmetry of the skeletal graphs, which however are two enantiomers (*cf.* Fig. 1*b*).

Finally, we would like to recall that PNS and PES representatives are based on simple but well chosen functions. Thus, changing the functions results in a change of PNS and PES which may be just a small deformation, a change of genus under preservation of significant geometrical features or a more or less complete reorganization of the shape. This makes them valuable tools for describing transformations between real structures, as we will show in the following.

2. Descriptions of phase transitions using periodic surfaces

Only a few attempts of correlating geometrical changes under RPT with PMS or PNS have been published hitherto. The

older zero-potential-surface approach (von Schnering & Nesper, 1987) was used to model the transition between the rocksalt and the caesium chloride structures (Oehme, 1989). By assigning the atomic sites of austenite to the flat points on the PMS D [corresponding to a face-centred cubic (f.c.c.) atomic arrangement] and by applying a transformation of the Bonnet type (Bonnet, 1853), a body-centred cubic (b.c.c.) structure arrangement that corresponds to the martensite lattice (Hyde, 1986; Hyde & Andersson, 1986) is formed at the end of a continuous deformation. The atomic positions were recovered from the flat points of the PMS gyroid. The gyroid surface appears as intermediate between the P and the D surfaces along the transformation. The Bonnet transformation is an isometric transformation, which means that it leaves all distances on the surface unchanged. Furthermore, most of the intermediate surfaces are self-intersecting and non-periodic. Such a transformation is thus very specific and topologically restricted because it does not allow for stretching or tearing of the surfaces during the change of geometry. This implies that Bonnet-type transitions are only possible between surfaces of the same genus. The embedding of networks on such surfaces and their transformations into each other thus applies only to very special cases controlled by the properties of the Bonnet transformation, which does not allow for connectivity changes. The topological description of solid–solid reconstructive phase transitions, which in general results in a severe reorganization of the structures involved, like changes in interatomic relations such as coordination numbers, bond neighbours, bond distances *etc.*, is still a great challenge. This is just what we are interested in modelling by our approach.

We are using the labyrinths of PES, chosen such as to envelope the network of the structures limiting the phase transition (Leoni, 1998) and finding intermediate envelope functions such that the path is as short as possible. The labyrinths of a PES are part of the same family of surfaces, which can be explored by the choice of the value of $f(x, y, z)$ in equation (3). For a set of function values but not for all $f(x, y, z)$, they have the same topological characteristic, *i.e.* the same genus as the distinguished surface, the PNS. We choose $f(x, y, z)$ such that the genus of the PNS is preserved and the network of interest is enclosed by a periodic surface, called an enveloping surface. This procedure is applied to both limiting structures, which determine the beginning and the end points of a RPT, respectively (Leoni, 1998).

The envelope functions are now very useful descriptors of atomic or group displacements, of bond rearrangements and of conformational changes involved in a phase transition. They reflect the deformation of a network by the change of the connectedness of the labyrinths measured by the variation of the genus. We interpret the change of the genus as the change of a chemical interaction, for example bond breaking. Qualitatively, the onset of a reconstruction becomes already visible in such a model in terms of narrowing of certain connections of the PES.

In summary, our approach works as follows:

(i) Definition of the envelope functions of the limiting structures by choosing the smallest set(s) of $\mathbf{S_h}$ such that the resulting PES show those characteristics of the structure one wants to analyse during the RPT, like the tetrahedral network of SiO_2 considered in this paper.

(ii) Linear interpolation of the two functions and PES calculation for each interpolation step.

(iii) Analysis of PES that exhibit change of the genus compared with the previous PES.

(iv) Recovery of atomic positions from the centres of the knots of the PES.

This procedure allows for an analysis of the change of the envelope functions quasi-continuously in arbitrarily small steps.

3. Phase transitions in the silica system

The phase system of the two most abundant elements in the outer earth shell, silicon and oxygen (Fig. 2), is remarkable for the many different structural variations based on tetrahedral motifs (Greenwood & Earnshaw, 1989). The normal-pressure high-temperature modifications β-quartz, β-tridymite and β-cristobalite are closely related to their low-temperature modifications α-quartz, α-tridymite and α-cristobalite, respectively. All of them are constituted of corner-linked tetrahedra. The change of symmetry during the α/β phase transitions of the displacive type can be described by group–subgroup relations. In the low-temperature α modifications, the tetrahedral SiO_4 units differ only in their mutual orientation compared with the β modifications. No change of coordination number or connectivity need occur. The way in which each pair α/β of phases is structurally related can easily be recognized by inspection.

The three high-temperature β modifications transform into each other on heating: The chiral network of quartz turns into the hexagonal network of tridymite and the latter finally into the cubic one of cristobalite before the system vitrifies. Despite the relatively simple looking networks, the transitions are of an interesting reconstructive character, requiring non-trivial rearrangements of the tetrahedral networks. This makes this system challenging and thus an excellent example for the applicability of the PES approach, especially to the RPT between the β modifications.

In the following sections, the PES approach is applied to the transition quartz to tridymite. Envelope functions are defined for both quartz and tridymite, and the model is a linear transition from one topology to the other.

4. The model of the tridymite structure

The high-temperature modification of tridymite crystallizes with the space-group symmetry $P6_3/mmc$. Along the c direction, the tetrahedra are corner connected in an 'eclipsed' manner and, in the other three directions, a 'staggered' sequence occurs, that is adjacent tetrahedra are rotated with respect to each other by 60°.

While for quartz a PNS was already available (von Schnering & Nesper, 1987, 1991), a suitable function for tridymite had still to be found. The first allowed $\mathbf{S_h}$ for this

space group is based on $\mathbf{h} = (10\bar{1}0)$; the full set of symmetry-equivalent vectors results in a PNS that represents a rod packing, developing parallel to the c axis in the symmetry-related channels of tridymite (Fig. 3*a*). Exploring different values of $f(x, y, z)$ allows one to define PES that clearly reveal the positions of the six- and threefold axes of the hexagonal space group. The translation parts of the matrices representing the space group do not affect the phases of this set. Addition

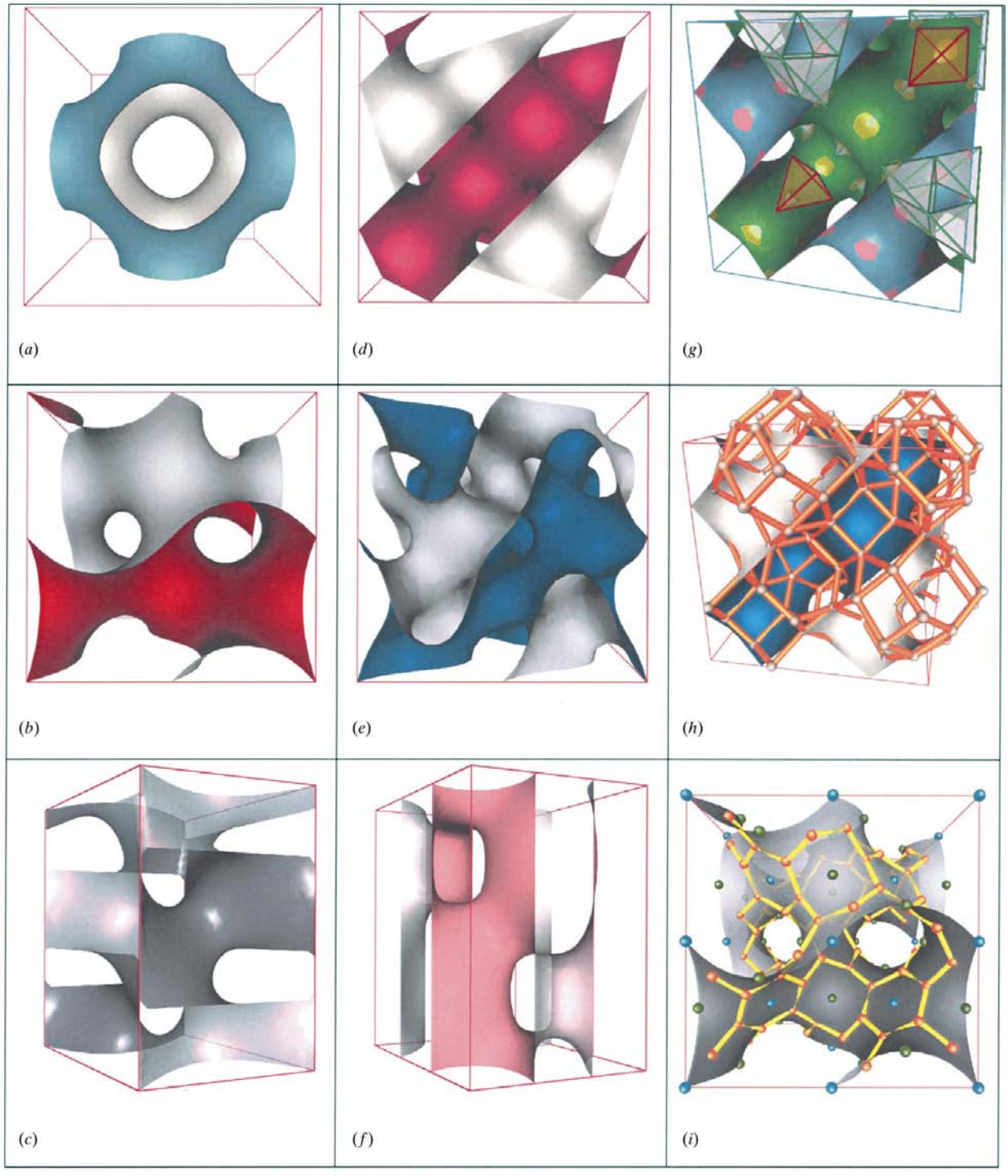

Figure 1
Examples of nodal surfaces (PNS) and selected correlations with crystal structures. (*a*) *P** surface (Schwarz's *P* surface) (Schwarz, 1890); (*b*) *Y*** surface (Schoen's gyroid surface) (Schoen, 1970); (*c*) *Q** surface representative for quartz-like double-helix structures; (*d*) *D** surface (Schwarz's *D* surface); (*e*) *S** surface (symmetry $Ia\bar{3}d$); (*f*) E–$00\frac{1}{2}E(P2z)_c$ surface (tridymite representation); (*g*) building blocks of $Li_5P_2N_5$ and *D** surface with P_4N_{10} unit exclusively in one tunnel system of *D**; (*h*) *D** and the Al framework of VAl_{10}; (*i*) *Y*** and the hypothetical *g*688 framework (Terrones & Mackay, 1997).

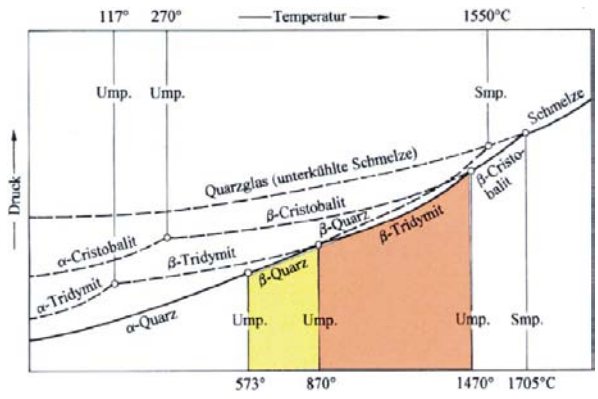

Figure 2
Part of the phase diagram of SiO_2. [Reproduced with permission from *Holleman-Wiberg Lehrbuch der Anorganischen Chemie* (1995). Copyright (1995) Walter deGruyter GmbH & Co.]

of the set $(10\bar{1}1, 1, 0)$, which is characteristic for the group owing to the specific phase permutations, causes the rods to connect to each other, thus forming a continuous triply periodic surface (Fig. 3*c*). One labyrinth is centred by the silica network and the correct alternation of 'eclipsed' and 'staggered' conformations appears clearly in the course of the PES along the [001] direction. The set $\mathbf{S_h}(10\bar{1}1, 0, 1)$ alone gives rise to a PNS with the symmetry $P6_3/mmc$ but with intersections along some special lines, corresponding to intersections of the *c* glide planes (Fig. 3*b*). Finally, addition of a third set of structure factors $(0002, 2 \times 2^{1/2}, \pi)$ provides for a PNS enveloping the network in the desired form (Fig. 3*d*). Now corresponding PES like the one in Figs. 3(*e*)–(*f*) surround the network in such a way that the tetrahedral shape and connectivity of the tetrahedra are approximated in a satisfactory way (Leoni, 1998).

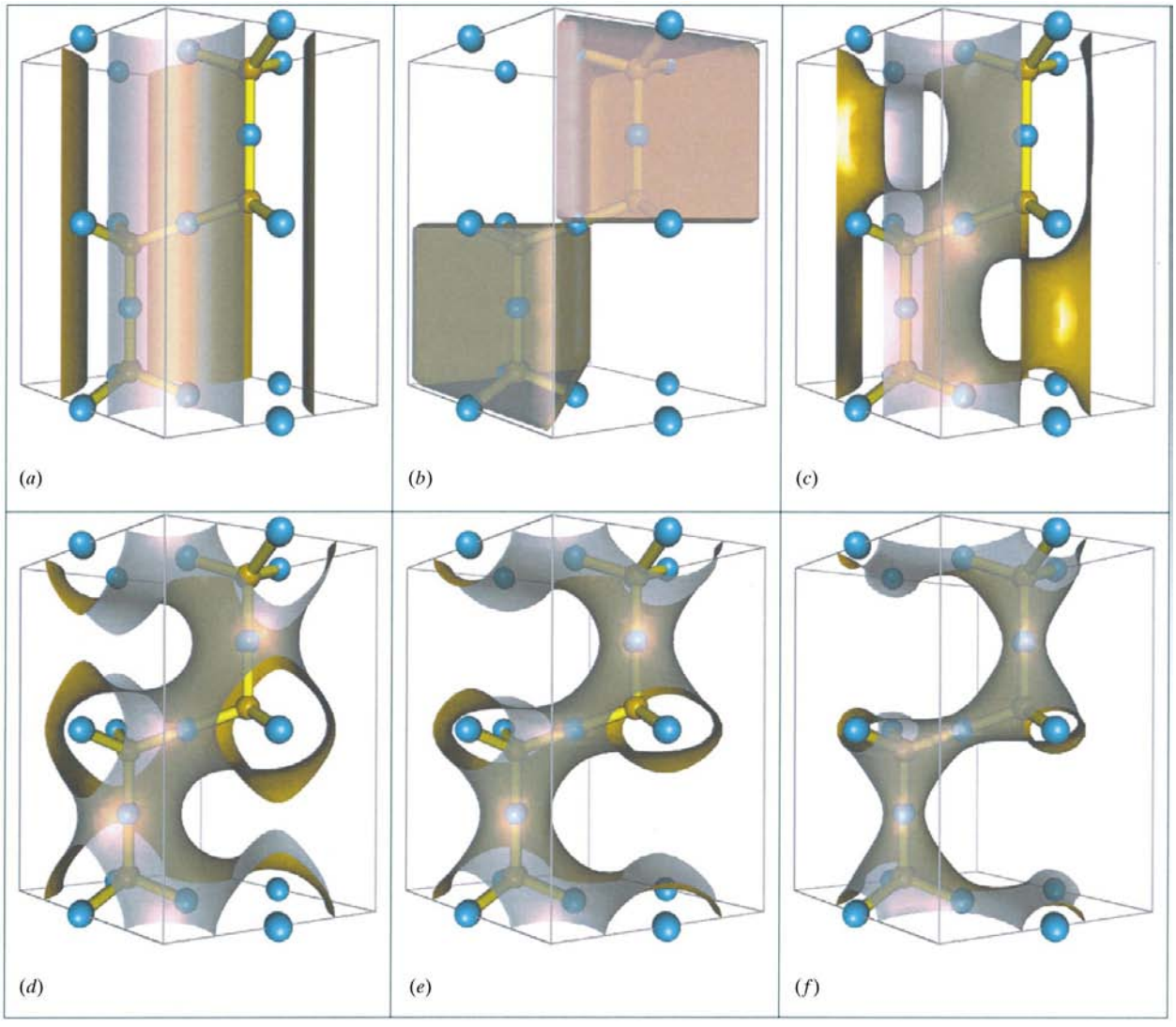

Figure 3
Construction of the tridymite representation: (*a*) PNS of the structure-factor set $(10\bar{1}0, 1, 0)$; (*b*) PNS of the structure-factor set $(10\bar{1}1, 1, 0)$; (*c*) PNS of the structure-factor sets $(10\bar{1}0, 1, 0; 10\bar{1}1, 1, 0)$; (*d*) PNS of the structure-factor sets $(10\bar{1}0, 1, 0; 10\bar{1}1, 1, 0; 0002, 2 \times 2^{1/2}, \pi)$; (*e*) PES of the set given in (*d*) for $f(x, y, z) = -1.5$; (*f*) PES of the set given in (*d*) for $f(x, y, z) = -3.0$.

An alternative representative may be gained with $\mathbf{S_h}(11\bar{2}0, 1, 0)$. The resulting PNS appears again as a rod packing, where the rods are centred on the geometrical positions of sixfold and threefold symmetry elements. Exploration of the PES functions allows one to discover a Kagomé net, appearing on fusing the rods. The oxygen positions of high-temperature tridymite correspond to the cross points of this net. Addition of the set $(10\bar{1}1, 1, 0)$ to the set $(10\bar{1}2, 1, 0)$ generates a PNS of more convoluted shape, with new channels opened in the primer tetrahedral framework representative. However, the PES of this function show additional features, *i.e.* another set of channels that obscures the simplest picture of the tridymite structure we are aiming at. That is why we do not consider this function further on in this work.

5. The model of the quartz structure

The chiral framework of β-quartz is described in the space group $P6_222$, enantiomorphous to $P6_422$. Its topology can very simply be described by the set $(10\bar{1}1, 1, 0)$, as already shown (von Schnering & Nesper, 1991). The resulting PNS, the so-called Q^* surface, separates two equivalent point configurations of the ^+Q lattice complexes from each other and is a fundamental representation of a four-connected network arranged in a hexagonal space group. In the real structure, the Si atoms occupy a point configuration of a ^+Q lattice complex, just leaving space for another point configuration of ^+Q, the two of which interpenetrate without being connected to each other but are separated by the PNS Q^*. The two point configurations are shifted against each other by $\mathbf{t} = (0, 0, 1/2)$. Again, the congruence of the subspaces assigns Q^* to the supergroup $P6_422$ (von Schnering & Nesper, 1991).

The PNS representation beautifully shows the interplay of 6_2 and 3_1 screw axes in the form of a continuous topological object (Fig. 1*c*, standard setting). The addition of a second set $(10\bar{1}0, 1, 0)$ allows for a better approximation of the network of quartz and of the tetrahedral building units that can now easily be visualized with suitably chosen PES (*cf.* Fig. 4*f*). We have chosen this as representative of the quartz structure.

Although the set $(10\bar{1}0, 1, 0)$ could be neglected without changing the desired enveloping function very much, it is necessary for the tridymite envelope and thus provides a better comparison of the sets.

In Table 1, phase relations and indices for the common supercell (*cf.* §6) exhibit nicely the difference in phase permutations starting from a symmorphic supergroup ($P6/mmm$) to $P6_3/mmc$ and $P6_222$, respectively. In the latter case, the screw symmetry is clearly reflected by the phase shifts.

6. Preparation of the phase-transition model

The structural problem of a RPT may be split into two transformations and treated separately although both of them belong together and proceed in parallel in real systems: (i) the mutual correlation of the unit cells of the two limiting structures; (ii) the topological changes of the building blocks inside the unit cells. Our approach utilizes the evaluation of a common supercell allowing for an integer multiple of the two different unit-cell contents. The mutual orientation is chosen according to topological and symmetry arguments, which in the case presented here are more or less congruent. This is different from Toledano *et al.* (Dmitriev *et al.*, 1998) who quite recently presented an interesting transition model based on a hypothetical b.c.c. aristotype structure (Bärnighausen, 1980).

Table 1
Indices and phases $\alpha_{\mathbf{h}}$ for the structure-factor set $(10\bar{1}1, |\mathbf{S_h}|, \alpha_{\mathbf{h}})$ in the symmetry groups of the supercell $P6/mmm$, $P6_3/mmc$ and $P6_222$.

$P6_3/mmc(c' = 3c)$ and $P6_222(c' = 4c)$ are isomorphic subgroups of $P6_3/mmc(c)$ and $P6_222(c)$, respectively.

Basis set	$P6/mmm$	$P6_3/mmc$ tridymite		$P6_222$ quartz	
$10\bar{1}1$	0	$10\bar{1}3$	0	$10\bar{1}4$	0
$1\bar{1}01$	0	$1\bar{1}03$	π	$1\bar{1}04$	$2\pi/3$
$0\bar{1}11$	0	$0\bar{1}13$	0	$0\bar{1}14$	$4\pi/3$
$\bar{1}011$	0	$0\bar{1}13$	π	$0\bar{1}14$	0
$\bar{1}101$	0	$\bar{1}103$	0	$\bar{1}104$	$2\pi/3$
$01\bar{1}1$	0	$01\bar{1}3$	π	$01\bar{1}4$	$4\pi/3$

Clearly, the two space groups involved in the RPT are not connected by a direct group–subgroup relation. Although in principle an infinity of different mutual orientations of the two unit cells are possible, we have chosen the one where the two unique axes are collinear. Matching the two unit-cell contents requires a fourfold quartz and a threefold tridymite cell, which is easily achieved by corresponding multiples of the c axes ($c'_{\text{quartz}} = 4 \times 5.460 = 21.880$; $c'_{\text{tridymite}} = 3 \times 8.220 = 24.660$ Å), while the bases are relatively unaffected ($a_{\text{quartz}} = 5.010$; $a_{\text{tridymite}} = 5.030$ Å).

The corresponding transformation matrices are

$$\mathbf{T}_{\text{quartz}} = \begin{vmatrix} 1 & 0 & 0 \\ 0 & 1 & 0 \\ 0 & 0 & 4 \end{vmatrix}$$

and

$$\mathbf{T}_{\text{tridymite}} = \begin{vmatrix} 1 & 0 & 0 \\ 0 & 1 & 0 \\ 0 & 0 & 3 \end{vmatrix}$$

and the corresponding supercell contains 12 SiO_2 units.

Interestingly, the [001] screw vectors of the screw axes become $\frac{1}{12}c'$ for the 6_2 and $\frac{1}{6}c'$ for the 6_3 operations, which different orientations of the tetrahedra cannot account for because the largest length difference in a tetrahedron occurs on changing from the [100] to the [111] expansion if the tetrahedron matches to one half of the vertices of a cube (cube axes along [100], [010], [001]). Interestingly, this length change amounts to 1.15% while the difference for the c' axes of quartz and tridymite is 1.12% and thus very similar but just occasional because corresponding tilting of tetrahedra in the network cannot induce a transition from a helix with pitch of $\frac{1}{12}$ to one of $\frac{1}{6}$. Consequently, a reconstruction of the 3D frameworks by a bond-breaking mechanism is unavoidable in this

mutual setting of unit cells. Thus, the RPT has to include a bond-breaking mechanism and a severe lowering of the symmetry on the transition pathway.

We would like to point out that a doubling of the hexagonal bases allows for another supercell which is commensurate with cristobalite in trigonal setting as well. This cell contains 48 SiO_2 units. An RPT model based on this cell (Leoni, 1998) will be described in a subsequent paper.

As we *a priori* do not know how lattice constants should change under such a transition, there are only two simple possibilities: either to keep the cell volume or to interpolate linearly between the limiting axes. As the difference occurs mainly for c' and is fairly small, even a constant cell volume should do for an inspection of the RPT.

A very important task for the preparation of the transition model is the mutual location of origins of the basic unit cells, in other words the shift of the symmetry elements between the two limiting structures. This is achieved by a proper choice of the phase factors α of the structure factors $\mathbf{S_h}$. We discuss this problem with the structure factor $S_{10\bar{1}1}$: choosing $\alpha_{\text{tridymite}}(10\bar{1}1) = 0, \pi$ and $\alpha_{\text{quartz}}(10\bar{1}1) = 0, 2\pi/3, 4\pi/3$ superimposes the two sixfold axes but allows for six different mutual shifts along [001] according to the six possible phase combinations.

However, all six combinations give rise to essentially the same topological result, as we will show in the following. Table 2 contains the complete sets of structure factors that are used in the transition model. The sum of the weights of the reflections are chosen to be the same for both structures, eventually by multiplying one of the functions by a factor accounting for consideration or not of the (0006) set. At this point, we are ready to perform the phase transition by variation of a single parameter, the mixing ratios of the two limiting functions.

Table 2
Sets of structure factors used for the transition model.

	$P6_3/mmc$ tridymite	$P6_222$ quartz
$10\bar{1}1$	$(20\bar{2}3, 1, 0)$	$(20\bar{2}4, 1, 0)$
$10\bar{1}0$	$(20\bar{2}0, 1, 0)$	$(20\bar{2}0, 1, 0)$
0002	$(0006, 2 \times 2^{1/2}, \pi)$	–

7. Quartz-to-tridymite transition

The mixing is realized as weighted addition of the two basis functions for quartz and tridymite in steps of 10% according to the equation

$$f(\text{transition}) = vf(\text{quartz}) + (1 - v)f(\text{tridymite})$$
$$(v = 0, 0.1, 0.2, \ldots, 1.0).$$

The display of the resulting representations is given in Figs. 4(*a*)–(*f*). The PES for $f(x, y, z) = -3.0$ is displayed for each step. A corresponding ball-and-stick model for each intermediate structure results if an Si atom is placed at the centre of the knots of the labyrinths.

The centres are evaluated by contracting the PES, *i.e.* by increasing $|f(x, y, z)|$ until a reasonable envelope function is produced. In this context, reasonable means that the PES representatives of a structure – as we define them here – are only approximate envelopes of the observed geometry. For example, the function for tridymite given in Table 2 allows one to localize the Si position at 1/3 2/3 0.071 while the experimental data transformed to this setting are 1/3 2/3 0.0625 (Sato, 1964). This leads to a difference in the Si—O—Si separation of 0.19 Å (2.89 *versus* 3.08 Å, respectively).

After the functions have been mixed in the proportion 90% tridymite to 10% quartz, the tetrahedral networks opens at $\frac{1}{4}$ of all links (one Si—O—Si connection at each Si centre) and thus a change of the genus of the PES occurs. The Si—Si vectors that are disected are parallel to the direction [631] and its symmetry-related directions based on the tridymite symmetry. However, at a given level in z all broken connections are parallel, *i.e.* broken connections along [631], $[\bar{9}61]$, $[3\bar{9}1]$ occur at different layers in z, respectively. Changing the phase angle $\alpha(S_{10\bar{1}1})$ from 0 to $2\pi/3$ or $4\pi/3$ interchanges the direction-to-z correlation accordingly. Thus, $\frac{1}{4}$ of all connections are broken, one connection at each silicon centre. In other words, one of the connections becomes rapidly longer in this model while the other three connecting vectors are moving towards a common plane with the central silicon site. At the transition point – at 50%:50% mixing ratio – this site has a trigonal planar coordination. Beyond this point, the local geometry around the silicon sites approaches the tetrahedral coordination of the quartz structure. Locally, the whole RPT model consists of an inversion at each silicon centre. This kind of local transformation is referred to as an S_N2 reaction in chemistry.

8. The transition framework

The intermediate structure deserves special attention. As was mentioned previously, the opening of a bond at each tetrahedral centre gives rise to a 3-connected network, consisting of 10-gons. If we only focus on the Si sites, then this kind of network is similar to the tetragonal silicon network found in α-$ThSi_2$. In fact, both the intermediate and the α-$ThSi_2$ structures contain a set of zigzag chains that are linked to form a 3D net (*cf.* Fig. 5*a*). After Wells, the net is of the (10, 3)-*b* type. In the tetragonal net, consecutive chains along [001] are rotated by 90° against each other (Wells, 1991). The idealized net formed by the boron atoms in B_2O_3 at ambient pressure is of type (10, 3)-*c*. It is built up by the same type of zigzag chains but rotated by 120° with respect to each other along [001] (*cf.* Fig. 5*b*). In the real structure, the planes of the zigzag chains are tilted away from the [001] zone as shown in Fig. 5(*c*), which reduces the symmetry to $P3_1$. In our transition intermediate (Fig. 5*d*), the angles for the tilting of the chains around [001] are such that only a $P2_1$ symmetry remains for the supercell. According to the three decomposition possibilities of the

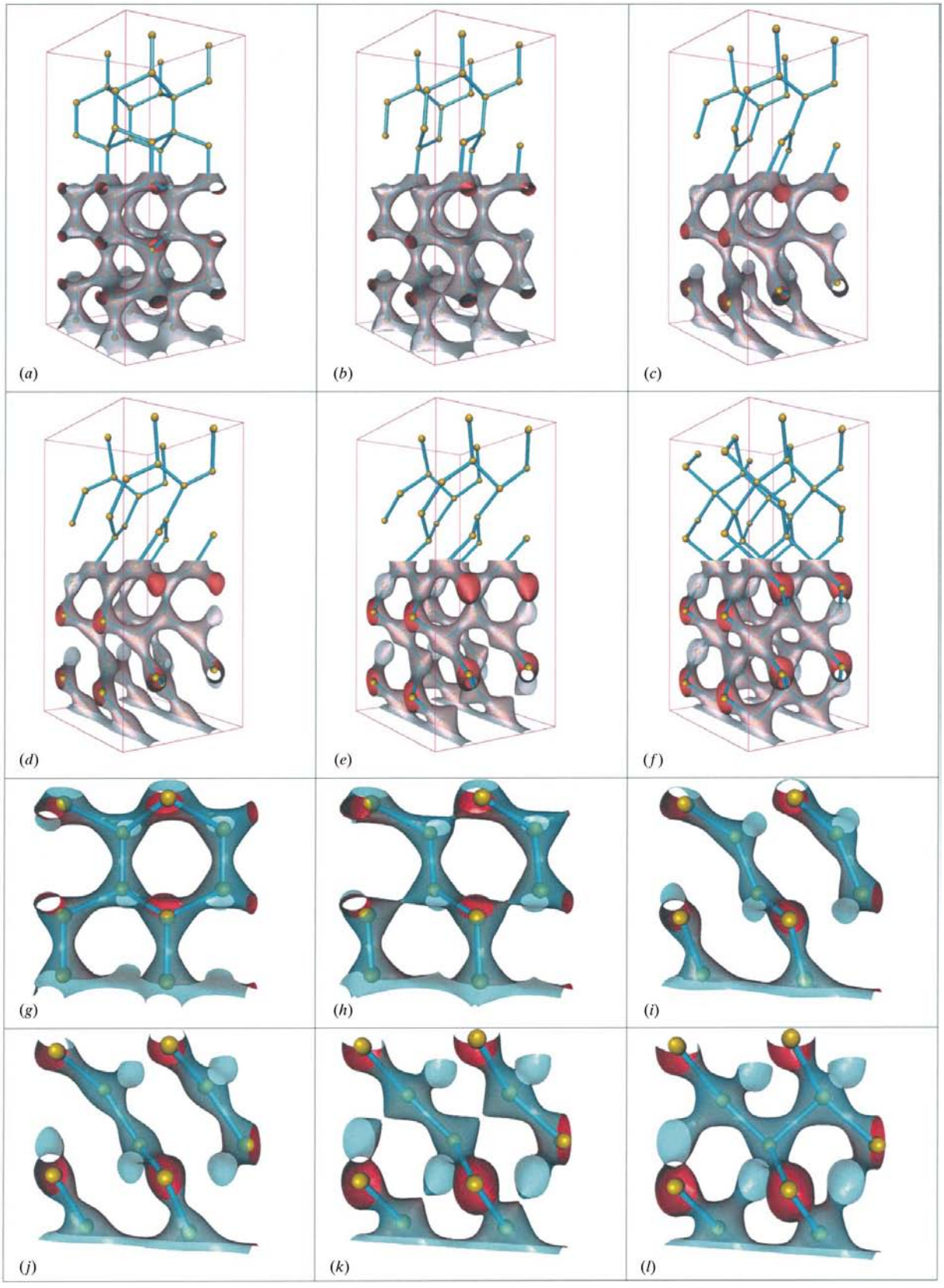

Figure 4
PES model of the phase transition and stick-and-ball arrangements recovered from the corresponding surface representations: (*a*) tridymite structure and PES for $f(x, y, z) = -3$; (*b*) linear mixing of tridymite and quartz representatives (90%:10%) – one Si—O—Si connection per Si centre is already lost; (*c*) transition state with trigonal planar nodes for a mixing ratio of 50% tridymite to 50% quartz; (*d*), (*e*) linear mixing of tridymite and quartz representatives at 40%:60% and 10%:90% mixing ratio – recovery of the pyramidal conformation; (*f*) quartz structure and PES for $f(x, y, z) = -3$. The missing fourth Si—O—Si connection per Si centre has been re-established. The net geometrical change is an inversion at each silicon centre, which, however, does not directly explain possible pathways of the O atoms. (*g*)–(*l*) Detail of the formal inversion at a silicon centre.

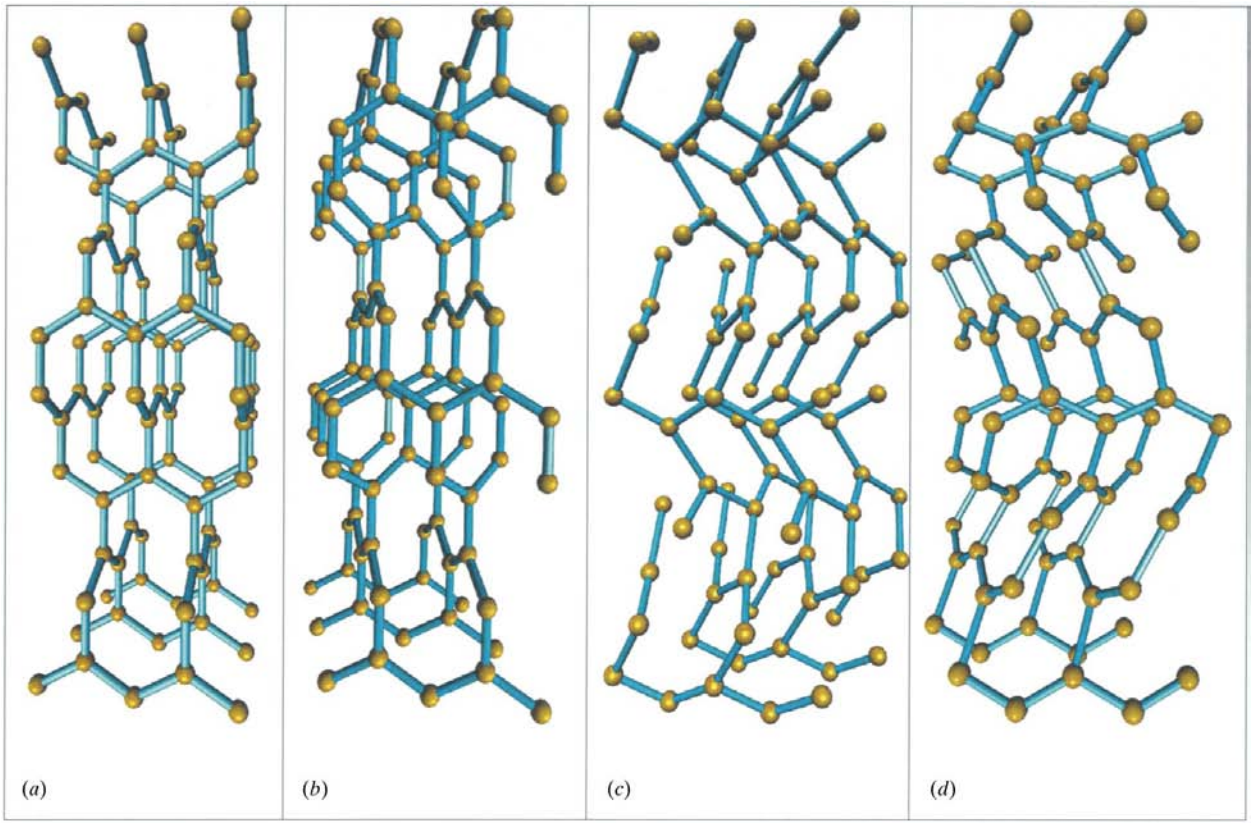

Figure 5
Comparison of the intermediate structure with known structural types. (*a*) (10, 3)-*b* net of symmetry $I4_1/amd$, corresponding to the silicon net in tetragonal α-$ThSi_2$. (*b*) (10, 3)-*c* net of symmetry $P3_112$. (*c*) Net formed by the B atoms in trigonal B_2O_3, symmetry $P3_1$. (*d*) Intermediate transition structure. The cell choices for B_2O_3 and for the intermediate have been adapted to allow a better comparison with the ideal models.

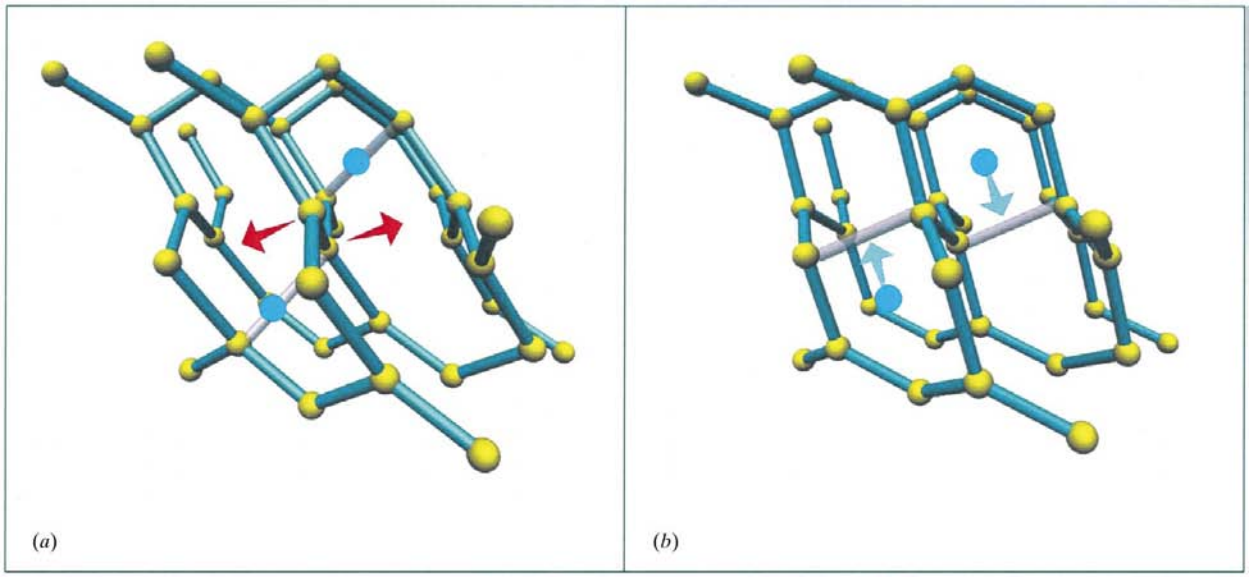

Figure 6
Concerted transition model for the O atoms going from the quartz to the tridymite structure. Two steps close to the intermediate structure are displayed, corresponding to a mixing of tridymite and quartz representatives at (*a*) 30%:70% and (*b*) 70%:30%. Two connections representing Si—O—Si bonds in the limiting structures are visible. The movement of the silicon network as it is calculated in this paper (orange arrows), causing the opening of large voids, and the correlated movement of O atoms (blue circles) according to the bright blue arrows allows for a five-coordinated transition state at each silicon centre. This would energetically be much more favourable than the triply coordinated one (no complete breaking of bonds).

hexagonal to monoclinic symmetry, there are three such equivalent solutions for the intermediate.

9. Comparison with other RPT models

To our knowledge, a RPT model for the quartz-to-tridymite conversion as presented here has not been proposed before. As mentioned in the beginning, there are very interesting models by Toledano *et al.* (Dmitriev *et al.*, 1998) and by Jacob *et al.* (Jacob, 1994; Lidin *et al.*, 1992). In the approach by Toledano, a b.c.c. structure is defined as a common aristotype. All transformations between SiO_2 modifications and the b.c.c. structure are analysed and some combined transformations according to modification $a \rightarrow$ b.c.c. $\rightarrow$ modification b are explored but not the quartz–tridymite transition. In any case, there is a marked difference between their approach and ours: (i) the mutual orientations of quartz and tridymite in the b.c.c. 'subcell' do not arrange the unique axes in a collinear fashion; (ii) the necessary distortions of the unit cells are much larger *via* the b.c.c. parent structure than in our case; (iii) they do not give a quantitative topological analysis of how the SiO_2 framework would change locally under the RPT, although some conjectures on the structure of the transition intermediates are given.

The RPT model of Jacob *et al.* implements a so-called local bond-flip mechanism. The RPT is achieved by a breaking and a reformation of a total of six bonds per one double tetrahedron $O_{3/2}Si-O-SiO_{3/2}$ in connection with a rotation of this group. Although a more economical way may be derived by a different rotation and a breaking of a total of four bonds, it is still even in this respect very much different from our model where only one bond per $SiO_{4/2}$ group is reconnected.

10. Consideration of the oxygen migration

As the oxygen centres are not explicitly included, for the reasons mentioned, we cannot follow their behaviour in our model as defined above. Although one could expand the Fourier series with respect to a proper location of the oxygen positions in the limiting structures, one would lose the simplicity of the topological description. In any case, as long as the functions do show tetrahedral connections, an oxygen is unambiguously localized in the tunnel connecting two Si centres. However, cutting the latter will not allow for a geometrical localization of the O atoms any more, as the model accounts only for the variation of connectedness at the silicon centres and for their displacement.

Assuming the movement of the Si centres is reasonable, we can search for shortest oxygen migration ways in the silicon framework of the model. Our result is a two-O-atom four-centre transition path, which is displayed in Figs. 6(*a*)–(*b*). The O atoms are indicated by small spheres between the silicon nodes and their most probable migrations are referred to by the straight arrows. The O—O repulsion would effectively lead to a rotation of SiO_4 tetrahedra around Si centres. This type of transition would proceed *via* a fivefold local transition coordination.

11. Conclusions

A topologically simple and short transition mechanism for the RPT between quartz and tridymite has been derived utilizing periodic nodal (PNS) and equi-surfaces (PES) as transition descriptors between the limiting structures of the two phases. These descriptors, called structure representatives, can easily be developed from the Fourier transforms of short but characteristic series of selected structure-factor sets of a common supercell of the limiting structures. Linear interpolation between the limiting PES functions allows for a continuous topological transition. Changes of the genus during the transition are interpreted as severe reconstruction, *i.e.* bond breaking which may accompany the continuous distortions of the representatives along the transition path. Relevant positional parameters are recovered from selected PES for large absolute function values which correspond to cross-linking parts or knots of the continuous representatives at lower absolute function values. Analysis of both the combined structure-factor sets of the limiting structures and the changes of the real-space coordinates allows for a detailed symmetry analysis (picture?) of the transition model. Although starting from either of the limiting structures the symmetry markedly decreases, the continuous nature of the model allows one to derive mutual atomic movements for the whole transition. The RPT model presented is not necessarily meant to describe a collective transition of large domains but may just account for the possibility of topologically short and effective local distributions and reconstructions.

It should finally be noted that this RPT model may not correspond to the pathway of lowest energy, especially because of the periodic nature of the *Ansatz* leading to a large number of excitations that had to be performed simultaneously. Thus, the continuous cooperative and periodic transition model presented is a study of the topological feasibility of a short or simple transition pathway. The same *Ansatz* has been applied to other RPT and the results will be presented in subsequent papers.

We would like to thank Dr Michael Jacob for helpful discussions. Our thanks are also extended to two anonymous reviewers for their helpful comments on an early version of this paper. The support of the Swiss National Science Foundation under project No. 2000-050675 is gratefully acknowledged.

References

Andersson, S., Hyde, S. T. & von Schnering, H. G. (1984). *Z. Kristallogr.* **168**, 1–17.
Andersson, S. & Jacob, M. (1997). *The Mathematics of Structures.* München: Oldenbourg.
Andersson, S. & Jacob, M. (1998). *The Nature of Mathematics and the Mathematics of Nature.* Amsterdam: Elsevier.
Bärnighausen, H. (1980). *Match*, **9**, 139–175.
Bonnet, O. (1853). *C. R. Acad. Sci.* **37**, 529–532.
Chen, C.-C., Herhold, A. B., Johnson, C. S. & Alivisatos, A. P. (1997). *Science*, **276**, 398–401.

Dmitriev, V. P., Toledano, P., Torgashev, V. I. & Salje, E. K. H. (1998). *Phys. Rev. B*, **58**, 11911–11921.
Faelth, L. & Andersson, S. (1982). *Z. Kristallogr.* **160**, 313–316.
Greenwood, N. N. & Earnshaw, A. (1989). *Chemistry of the Elements*, p. 393. Oxford: Pergamon Press.
Holleman-Wiberg Lehrbuch der Anorganischen Chemie (1995). Berlin: deGruyter.
Hyde, S. T. (1986). PhD thesis, Monash University, Australia.
Hyde, S. T. & Andersson, S. (1984). *Z. Kristallogr.* **168**, 221–254.
Hyde, S. T. & Andersson, S. (1986). *Z. Kristallogr.* **174**, 225–236.
Hyde, S. T., Andersson, S., Larsson, K., Blum, Z., Landh, T., Lidin, S. & Ninham, B. W. (1997). *The Language of Shape.* Amsterdam: Elsevier.
Jacob, M. (1994). PhD thesis, University of Lund, Sweden.
Landau, L. D. & Lifshitz, E. M. (1959). *Statistical Physics.* Oxford: Pergamon Press.
Leoni, S. (1998). PhD thesis No. 12783, ETH Zurich, Switzerland.
Lidin, S., Andersson, S., Fogden, A., Jacob, M. & Blum, Z. (1992). *Aust. J. Chem.* **45**, 1519–1526.
Oehme, M. (1989). Dissertation, University of Stuttgart, Germany.
Parthé, E. (1995). TYPIX – Database of Inorganic Structure Types, Université de Genève, Switzerland.
Sato, M. (1964). *Mineral. J.* **4**, 115–130.
Schnering, H. G. von (1993). Unpublished results.
Schnering, H. G. von & Nesper, R. (1985). *Z. Kristallogr.* **170**, 138–140.
Schnering, H. G. von & Nesper, R. (1987). *Angew. Chem. Int. Ed. Engl.* **26**, 1059–1080.
Schnering, H. G. von & Nesper, R. (1991). *Z. Phys. B*, **83**, 407–412.
Schoen, A. H. (1970). *Infinite Periodic Minimal Surfaces without Self-Intersections*, *NASA Technical Note* No. D5541.
Schwarz, H. A. (1890). *Gesammelte Mathematische Abhandlungen.* Berlin: Springer.
Shmueli, U. (1993). *International Tables for Crystallography*, Vol. B, edited by U. Shmueli, ch 1.4. Dordrecht: Kluwer Academic Publishers.
Terrones, H. & Mackay, A. L. (1997). *Prog. Cryst. Growth Charact.* **34**, 25–36.
Toledano, P. & Dmitriev, V. (1996). *Reconstructive Phase Transitions in Crystals and Quasicrystals.* Singapore: World Scientific.
Wells, A. F. (1991). *Structural Inorganic Chemistry.* Oxford: Clarendon Press.
Zürn, A. (1998). PhD thesis, MPI Stuttgart, Germany.